

Unveiling the Achilles' Heel: Backdoor Watermarking Forgery Attack in Public Dataset Protection

Zhiying Li, Zhi Liu, Dongjie Liu, Shengda Zhuo, Guanggang Geng, Jian Weng, Shanxiang Lyu, and Xiaobo Jin

Abstract—High-quality datasets can greatly promote the development of technology. However, dataset construction is expensive and time-consuming, and public datasets are easily exploited by opportunists who are greedy for quick gains, which seriously infringes the rights and interests of dataset owners. At present, backdoor watermarks redefine dataset protection as proof of ownership and become a popular method to protect the copyright of public datasets, which effectively safeguards the rights of owners and promotes the development of open source communities. In this paper, we question the reliability of backdoor watermarks and re-examine them from the perspective of attackers. On the one hand, we refine the process of backdoor watermarks by introducing a third-party judicial agency to enhance its practical applicability in real-world scenarios. On the other hand, by exploring the problem of forgery attacks, we reveal the inherent flaws of the dataset ownership verification process. Specifically, we design a Forgery Watermark Generator (FW-Gen) to generate forged watermarks and define a distillation loss between the original watermark and the forged watermark to transfer the information in the original watermark to the forged watermark. Extensive experiments show that forged watermarks have the same statistical significance as original watermarks in copyright verification tests under various conditions and scenarios, indicating that dataset ownership verification results are insufficient to determine infringement. These findings highlight the unreliability of backdoor watermarking methods for dataset ownership verification and suggest new directions for enhancing methods for protecting public datasets.

Index Terms—Dataset protection, backdoor attack, data privacy, data security, AI security.

I. INTRODUCTION

High-quality datasets form a crucial foundation for artificial intelligence, as evidenced by the rapid development of large models (e.g., GPT [1], LLaMA [2]). However, constructing these datasets is an expensive and time-consuming process involving data collection, annotation, and cleaning [3]–[7]. This complexity makes public datasets a target for unethical companies or individuals seeking to enhance model performance to achieve quick profits, which in turn dampens

This work is partially supported by Research Development Fund with No. RDF-22-01-020, the top talent award project RDF-TP-0019 and National Natural Science Foundation of China under Grant U1804159. (Corresponding author: Shanxiang Lyu and Xiaobo Jin)

Zhiying Li, Zhi Liu, Dongjie Liu, Shengda Zhuo, Guanggang Geng, Jian Weng and Shanxiang Lyu are with College of Cyber Security, Jinan, University, Guangzhou 511436, China (email: {tzezd2019@stu2020., djliu@., gggeng@., lxx07@}jnu.edu.cn, {peterliuforever, zhuosd96, cryp-tjweng}@gmail.com).

Xiaobo Jin is with the School of Advanced Technology, Xi'an Jiaotong-Liverpool University, Suzhou 215000, China (email: xiaobo.jin@xjtlu.edu.cn).

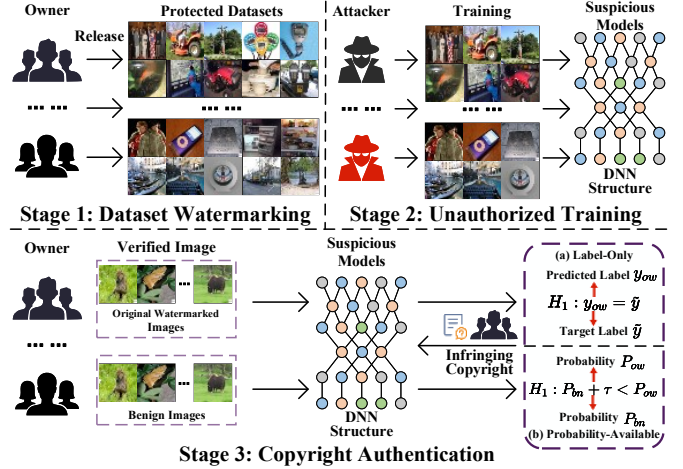


Fig. 1. Overview of backdoor watermarking. **Stage 1:** The dataset owner releases a watermarked dataset with target labels to the public (protected public dataset). **Stage 2:** The attacker uses the protected dataset to train a deep learning network without permission and provides a model API for query. **Stage 3:** The dataset owner queries the model API for responses to the original watermarked images and benign images, and determines copyright infringement through hypothesis testing methods.

the enthusiasm of members of the open-source community. Concerns have arisen regarding their datasets being used for purposes beyond education or research, including illegal activities, prompting greater caution in releasing datasets to the public. Consequently, the protection of public datasets is becoming an urgent and widely recognized issue [8]–[12].

Most dataset protection methods [13], [14] always focus on private datasets, such as encryption [15], [16], digital watermarking [17], [18], and differential privacy [17], [18]. These methods generally verify copyright and protect data by embedding encryption keys [19], unique watermarks [20] in the data, and controlling the model training process [20], allowing only authorized users to access, thereby reducing the risk of data theft. Since these methods require controlling the training process or affect the openness of the protected dataset (i.e., the public dataset), they are not applicable or suitable for public datasets. Compared with previous methods, backdoor watermarking provides necessary protection for public datasets from the perspective of data without affecting the openness of public datasets, and is therefore becoming a mainstream solution for public dataset protection. Backdoor watermarking redefines the protection of public datasets as a dataset ownership verification (DOV) problem [8]–[11], that is, dataset

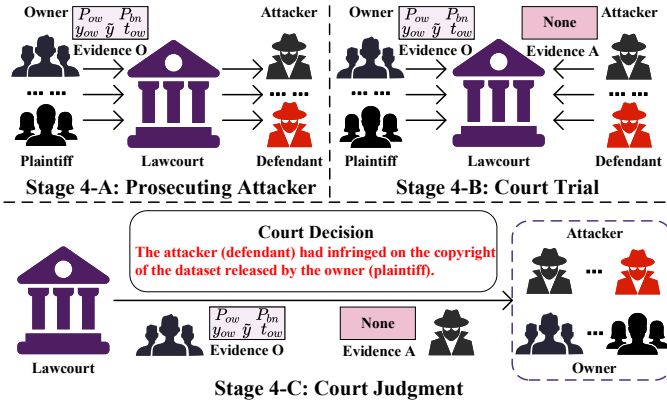


Fig. 2. The main process of the court judgment: **Stage 4A:** The dataset owner uses the evidence to sue the attacker in court and provides evidence (Evidence O in Figure) to the court, including the suspicious model’s response P_{ow} and P_{bn} to the original watermarked and benign images, the target label \tilde{y} , the predicted label y_{ow} , and the original watermark t_{ow} . **Stage 4B:** During the trial, the evidence provided by the dataset owner shows that the attacker has infringed the copyright, while the attacker cannot provide any evidence (Evidence A in the figure). **Stage 4C:** The court announces the final judgment: Since the attacker cannot provide any evidence, but the data owner provides sufficient evidence, the attacker has infringed the copyright.

owners can use a poison-only backdoor method [21]–[24] to watermark the dataset before publishing, and then verify ownership by detecting whether the trained model exhibits predefined backdoor behavior (as shown in Figure 1).

Despite the advantages of backdoor watermarking, the existing process remains overly simplified. The current algorithm ignores the existence of third-party judicial institutions (such as courts), and lacks a robust mechanism to ascertain infringement based on DOV results. Consequently, this limitation reduces its practicality in real-world applications. Specifically, the process implicitly assumes that the attacker (i.e., the model trainer) will sit back and wait when accused, and will not collect evidence and refute it in court. However, this assumption is not in line with reality. The attacker will try his best to find evidence to defend himself and provide rebuttal evidence to avoid being judged as an infringement. The DOV results obtained by the current backdoor watermarking method cannot accurately determine infringement. Based on the above analysis, we conclude that backdoor watermarking methods face two major challenges: **1) imperfect process; 2) non-robust DOV.**

To address the challenge of imperfect processes, we introduce third-party judicial institutions such as courts to make fair judgments. Ideally, the court judgment process includes three main stages (as shown in Figure 2): prosecuting attacker, court trial, and court judgment. First, the copyright owner (plaintiff) sues the attacker (defendant) for copyright infringement and submits evidence to the court, including the original watermark t_{ow} , the target label \tilde{y} , and the verification results P_{ow} , P_{bn} , and y_{ow} , as shown in Figure 1. Second, both parties submit evidence during the court trial and debate in court. Third, the court makes a judgment based on the evidence submitted by both parties. Throughout the process, accusations based on DOV results can gain greater credibility and legal effect.

Regarding the robustness challenge of DOV, we believe that

the DOV results are not robust from the perspective of forgery attacks. As different watermarks can produce the same verification results, this reveals that existing backdoor watermark-based DOV has significant security risks in protecting public datasets. Here are the main details:

- First, when attackers realize that they are being sued, they will make every effort to obtain the watermark information in the protected dataset. Attackers can use backdoor data detection methods to identify abnormal backdoor data at the model or data level [25]–[28]. By comparing and querying suspicious models, attackers can collect all watermark information in the protected dataset.
- Second, once the attackers have all the watermark information, they can conduct forgery attacks to provide rebuttal evidence. Inspired by these findings, we propose a new watermark forgery algorithm based on the idea of distillation learning from the attacker’s perspective. Specifically, assuming that there is an original watermark generator (which may not exist) that can generate the original watermark, called the teacher; we design a new **Forged Watermark Generator (FW-Gen)** based on the idea of encoding and decoding, called the student, and input the image containing the original watermark and the image containing the forged watermark into the classification model (benign model or watermarked model) respectively to obtain two probability distributions. The algorithm is driven by two distillation losses to optimize only the parameters of the forged watermark generator.
- Finally, the attacker submits rebuttal evidence to the court, including the forged watermark, the suspicious DNN’s response to the forged watermark, and the predicted label of the forged watermark image, which invalidates the owner’s evidence and successfully escapes the charges.

The key contributions of our work are as follows.

- We refine the process of backdoor watermarking for protecting public datasets by adding third-party judicial institutions (such as courts), making it more practical and applicable in real-world scenarios.
- In the field of public dataset protection, to the best of our knowledge, we are the first to reveal the backdoor watermarking vulnerability from the perspective of forgery attacks. Specifically, we develop a **Forgery Watermark Generator (FW-Gen)** that can forge the original watermark.
- Extensive experiments demonstrate the effectiveness of FW-Gen, where the forged watermark generated by FW-Gen is stylistically different from the original watermark but has the same functionality in activating the backdoor in the classification model.

II. RELATED WORK

Below we review related works on backdoor attacks and dataset protection.

A. Backdoor Attack

Backdoor attacks are currently an emerging area of research, where attackers attempt to embed hidden backdoors

into models during the training process. watermarked models behave normally on benign samples but behave abnormally on watermarked samples containing backdoor triggers. For instance, BadNets [21] employs pixel patches as triggers, enabling the trained watermarked model to perform well on benign samples but exhibits attacker-specific behavior when processing images with specific triggers. Blended [22] merges natural images with blended attacks, thereby increasing the efficacy of backdoor attacks. In addition, Trojan [24] introduces an attack that preserves accuracy on clean inputs but facilitates Trojan behavior with near-perfect accuracy rates.

With the development of backdoor attack, more methods with higher stealthiness are investigated. For example, steganography conceals triggers within the model by employing regularization techniques to create triggers of irregular shapes and sizes [23]. Triggers are crafted based on anomalies in the latent representations of the watermarked model, and discrepancies in these representations are reduced using triggering functions [29]. The adaptive perturbation techniques are applied to significantly enhance both the stealthiness of the attack and the adaptability of defense strategies [30].

Existing backdoor attack methods always follow a paradigm that the triggers used to train the watermarked model are the same as the triggers used to activate the hidden backdoor during inference.

B. Dataset Protection

Dataset protection is to protect data from unauthorized access, and its main strategies are usually divided into two categories: private dataset protection and public dataset protection.

Private Dataset Protection. Encryption [16], [19], a classic dataset protection method, secures sensitive information by allowing only authorized users with the decryption keys to decrypt it. Digital watermarking [18], [31] safeguards image ownership by embedding unique patterns without revealing data details to the public. Differential privacy [32], [33] protects individual sample membership information within a dataset by controlling the model training process. However, these methods are unsuitable for protecting public datasets due to their inherent accessibility.

Public Dataset Protection. Public dataset protection can be defined as dataset ownership verification (DOV) [8], aimed at verifying whether a given suspicious model has been trained using the public dataset. Since backdoor attacks allow customization of behavior upon activation, they have become the most suitable method for protecting public datasets. Poison-label backdoor attacks [8] watermark the public dataset by changing the samples' class labels to a target class. Clean-label backdoor attacks [10] watermark the protected dataset without altering the samples' class labels. However, because both methods introduce misclassification behavior, domain generalization is employed to enhance DOV, enabling the watermarked model to correctly classify some 'hard' samples [11].

Existing backdoor watermarking relies on the consistency of backdoor attacks for copyright authentication, and implicitly

make a strong assumption that the attacker will not refute the accusation. Inspired by these findings, we rethink the copyright authentication process from the perspective of forgery attacks, revealing significant security vulnerabilities.

III. PRELIMINARIES

In this section, we will provide a detailed description of the processes involved in backdoor watermarking, image classification, and dataset ownership verification with hypothesis testing.

A. Image Classification

In the supervised image classification task with deep learning, given an image x , our goal is to build a deep learning network or classification model f to output the posterior probability p of K classes:

$$f(x; \theta) = p \in [0, 1]^K, \quad (1)$$

where θ is the parameter of the deep learning network. In order to determine the unknown parameter θ of the model, in the training stage, we collect a large number of images and assign labels to them to obtain a training dataset $D = (x_i, y_i)_{i=1}^N$. We then minimize the following objective function, known as empirical risk loss, to search for the optimal parameter θ^* :

$$\min_{\theta} \sum_{i=1}^N L(f(x_i; \theta), y_i), \quad (2)$$

where function L may be squared error loss or multi-class cross entropy loss. Once we get the optimal parameter θ^* , in the test stage, for any unknown sample x , we assign it to the category c with the largest posterior probability:

$$p = f(x; \theta^*), \quad c = \arg \max_{k=0,1,\dots,K-1} p_k, \quad (3)$$

where p_k represents the k -th component of the vector p . After the trained model is deployed online, the API provided to the public usually has the following two forms: *class probability distribution* $p \in [0, 1]^K$ or *predicted class label* $c \in [0, 1, \dots, K-1]$. Since the empirical risk loss function is a non-convex function and there is no global optimal point, stochastic gradient descent algorithm is usually used to find a local minimum point.

B. Backdoor Watermarking

We introduce backdoor watermarking in the field of image classification. Given a benign dataset $D = \{(x_i, y_i)\}_{i=1}^N$, where $x_i = [0, 255]^{C \times W \times H}$ represents the i -th image and $y_i \in \{0, 1, \dots, K-1\}$ is its corresponding label. The dataset owner selects a certain proportion of γ (watermark rate) of benign images from D to embed the watermark to obtain an original watermarked image and replace the benign image with it, while modifying its label y_i to the target label \tilde{y} , thereby obtaining a protected dataset \tilde{D} . In particular, Badnets [21] obtains a watermarked image \tilde{x}_i by weighted averaging the benign image x_i and the watermark t in an element-wise manner, that is, $\tilde{x}_i = (1-\rho) \odot t + \rho \odot x_i$, where $\rho \in [0, 1]$. Potential

attackers can use the protected dataset to train the classification model f without authorization, and then provided an API interface for external use. The data owner inputs n original watermarked images $\{\tilde{x}_i\}_{i=1}^n$ into the suspicious model f and obtains the predicted label $\{y_i\}_{i=1}^n$. Given n pairs of predicted labels and target labels $\{(y_i, \tilde{y}_i)\}_{i=1}^n$, at a given significance level α , the data owner uses statistical tests (e.g. T-test [34]) to determine whether the statistical hypothesis $f(\tilde{x}) \neq \tilde{y}$ holds and whether the suspicious model released by the attacker is infringing.

C. Copyright Verification with Hypothesis Testing

Paired T-test. Backdoor watermarking mainly considers two scenarios for protecting public datasets: **independent model scenario** and **stealing model scenario**. In the stealing model scenario, the target label \tilde{y} of the watermarked image is a label predefined by the dataset owner; while in the independent model scenario, its target label is the same as the label of the benign image. Below we take the **stealing model scenario** as an example to introduce the copyright verification process using the paired T-test [34].

When the model API outputs probabilities, then:

$$p = f(x), \quad \tilde{p} = f(\tilde{x}), \quad p, \tilde{p} \in [0, 1]^K, \quad (4)$$

where p and \tilde{p} represent the predicted probabilities of images x and \tilde{x} , respectively.

Assuming that the model uses the public data released by the data owner, the true labels of images \tilde{x} and x should be \tilde{y} and y ($y \neq \tilde{y}$) respectively. Note that according to Eqn. (3), we have:

$$p_{\tilde{y}} \leq p_y = \max_k p_k, \quad \tilde{p}_{\tilde{y}} = \max_k \tilde{p}_k. \quad (5)$$

Ideally, since the inputs x and \tilde{x} are very close, the two probability distributions p and \tilde{p} should also be very close. We have $p_{\tilde{y}} + \tau < \tilde{p}_{\tilde{y}}$, where τ is usually set to 0.2. There are two hypotheses as follows:

$$H_0 : p_{\tilde{y}} + \tau = \tilde{p}_{\tilde{y}}, \quad H_1 : p_{\tilde{y}} + \tau < \tilde{p}_{\tilde{y}}. \quad (6)$$

The data owner randomly chooses the output $(p_{(i,\tilde{y})} + \tau, \tilde{p}_{(i,\tilde{y})})_{i=1}^n$ of n pairs of benign samples and watermarked samples to conduct the one-sided paired T-test, where the confidence level α is 0.05. If hypothesis H_0 is rejected and hypothesis H_1 is accepted, the data owner will conclude that the dataset user has committed infringement.

Wilcoxon Signed-rank Test. The API provided by attackers usually has two forms: category probability distribution p or category label \tilde{c} , which are verified by **probability available verification** and **label only verification** [8] respectively. In particular, when the suspicious model only outputs the class label, the data owner can perform statistical tests on the prediction results and target labels through Wilcoxon signed-rank test to determine the infringement of the dataset.

When the model API outputs the class label, then there is:

$$\tilde{c} = f(\tilde{x}). \quad (7)$$

Assuming that the user uses the data published by the data owner, ideally, there should be $\tilde{c} = \tilde{y}$. Similarly, we can

randomly select n watermarked samples to perform the two-side Wilcoxon test, where the two assumptions are:

$$H_0 : f(\tilde{x}) \neq \tilde{y}, \quad H_1 : f(\tilde{x}) = \tilde{y}. \quad (8)$$

Here, rejecting H_0 means data copyright has been violated.

IV. THREAT MODEL

In this section, we will describe the threat model based on the goal, ability and knowledge of both defender and attacker. Note that the defender is the dataset owner, and the attacker is the suspicious model owner.

Defender Goal. The defender aims to protect the copyright of the datasets by embedding backdoor watermarks into protected datasets before releasing them to the public. The models trained with watermarked datasets should behave normally on samples without the aforementioned watermarks and abnormally on samples with watermarks, in order that DOV results can show that the attacker infringes the copyright of the public datasets.

Attacker Goal. The attacker aims to forge fake watermarks which can make the models watermarked by the watermarks from the defender behave as same as the watermarks from the defender when embedding into samples, in order that when the defender sues the attacker about infringing copyright, the attacker can provide evidence to defend himself.

Defender Ability. The defender has the full control of the public datasets, but can not access the target models. The defender can only query the models through the API function to confirm whether the attacker has committed data infringement. When the query results processed with DOV reach the threshold set by the defender, the dataset owner can determine that the attacker has infringed the copyright and submit evidence including the output values P_{ow} and P_{bn} of the original watermarked image and the benign image on the model, the target label \tilde{y} and the original watermark t_{ow} to the court for a fair judgment.

Attacker Ability. The attacker has the full control of the watermarked models, and can access the released public datasets. When accused by the defender, the attacker can inspect the released datasets and use them to construct fake watermarks.

Defender Knowledge. The defender has a complete understanding of the datasets and the watermarks with its corresponding target labels to protect the datasets. About the target model, although the defender has a comprehensive understanding of the original watermark t_{ow} and the target label \tilde{y} , in the face of potential attackers, the dataset owner has limited knowledge of the attacker's training process and model parameters.

Attacker Knowledge. First, the attacker has the complete knowledge of the watermarked models. Second, although the original watermark t_{ow} and target label \tilde{y} embedded by the dataset owner are confidential, attackers can still legally obtain this information. Specifically, when the attacker learns that he has been sued by the owner for copyright infringement, he will detect these watermarks through various methods

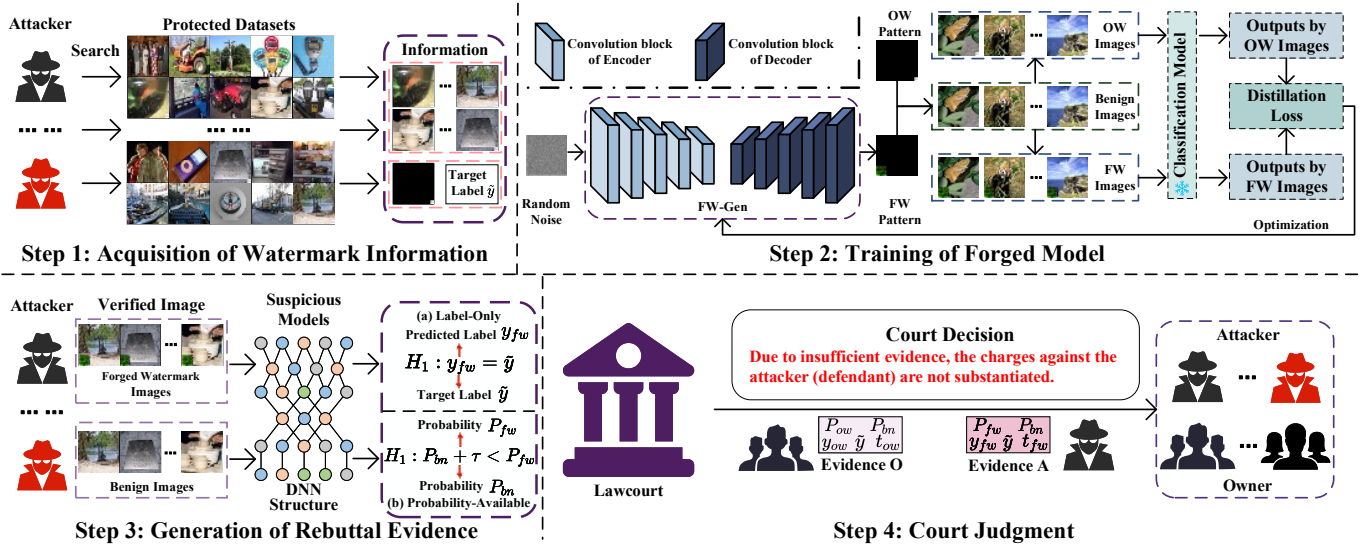


Fig. 3. The proposed forgery attack scheme is summarized, including several key steps: acquisition of watermark information, training of forged model, generation of rebuttal evidence and court judgment, where OW represents the original watermark and FW represents the forged watermark; evidence O includes the suspicious model’s response to the original watermarked and benign images (P_{ow} and P_{bn}), target label \tilde{y} , predicted label y_{ow} and original watermark t_{ow} ; evidence A includes the suspicious model’s response to the forged watermarked and benign images (P_{fw} and P_{bn}), target label \tilde{y} , predicted label y_{fw} and original watermark t_{fw} .

such as manual inspection and backdoor data detection¹. By testing the suspicious model trained on the protected dataset with samples with watermarks, the attacker can obtain the target label \tilde{y} . Third, the attacker can use this information to forge watermarks of different styles to replace the original watermark. The forged watermarks not only produce the same classification results, but also show consistent results in DOV. Finally, the attacker inputs the original watermarked image, benign image and forged watermarked image into the suspicious model to obtain their output values P_{ow} , P_{bn} and P_{fw} , which can be submitted to the court as evidence to refute the accusation. In general, with the limited knowledge of the protected datasets, the attacker can obtain information about the original watermark t_{ow} and the target label \tilde{y} to construct forged watermark.

V. REBUTTAL OF ATTACKER

In this section, we will describe how the attacker obtains the watermark, forges the model, generates rebuttal evidence and refutes the case in court from the attacker’s perspective, as shown in the four steps in Figure 3. In particular, we theoretically explain why the attacker can provide evidence by forging a backdoor watermark. In the above process, we proposed a new backdoor watermark forgery method, which aims to reveal the lack of robustness of the current DOV-based backdoor watermark and promote the development of public dataset protection.

A. Problem Definition

When the dataset owner sues the attacker for copyright infringement, he must provide the court with evidence including

¹Section VI-C verifies the feasibility of successfully obtaining watermark information.

the original watermark t_{ow} , the original watermarked image \tilde{x} , and the target label \tilde{y} . At the same time, the attacker can also legally obtain the watermarked dataset $\tilde{D} = \{(x_i, y_i)\}_{i=1}^N$, the original watermark t_{ow} , the original watermarked image \tilde{x} , and the target label \tilde{y} . The attacker can use this watermark information to forge the watermark t_{fw} so that the result of copyright verification is to accept the null hypothesis, thereby escaping the accusation of infringement. Below we will describe in detail the principle and process of how the attacker refutes the accusation.

B. Vulnerability of Backdoor Watermarking

We analyze the vulnerability of the above process from the perspective of adversarial training [35]. Adversarial training is an important way to enhance the classification model. It can not only improve the robustness of the model but also improve the returnability. Specifically, a robust model M is usually insensitive to the model input, which usually improves the generalization performance of the model, that is, the model satisfies the Lipschitz condition:

$$|f_M(x_1) - f_M(x_2)| \leq L(M) \|x_1 - x_2\|, \quad \forall x_1, x_2, \quad (9)$$

where $L(M)$ is a Lipschitz constant that depends on the model M . The target of adversarial training is to make the model still output the same results if the sample changes slightly. Therefore, we can conclude: **For the original watermark x_1 , there is at least another forged watermark x_2 that is different from it and behaves exactly the same as it on the model M , where it has some slight differences from the original watermark.**

C. Acquisition of Watermark Information

When the attackers learn that they are being sued for copyright infringement, they realize that there is a problem

with the dataset used for training, that is, the protected dataset may contain watermarks. At this point, the attackers face two choices: admit infringement or deny infringement. In reality, most attackers will choose to deny infringement for their own benefit and work hard to find rebuttal evidence.

For the target label, we directly input the backdoor watermark data into the suspicious model distributed by the attacker, and the output result is the target label.

For the watermark information, the attacker obtains it from the protected dataset by detecting abnormal data from the model or data level [25]–[28]. In our work, we use a frequency domain-based detection method [28], the core idea of which is that the existing backdoor watermark data usually shows anomalies in the high-frequency region, which usually corresponds to the backdoor watermark data. We strictly follow the operation process of [28], and the specific experimental details and detection results are shown in Section VI-C. The watermark information was successfully detected, which also shows a disadvantage of the current visible backdoor watermark. Therefore, developing invisible watermark algorithms will be a focus of future research.

Through the above process, the attacker can obtain watermark information such as the watermark, the original watermarked image, and the target label.

D. Training of Forged Model

We mainly introduce the process of generating forged watermarks after obtaining all watermark information, including network architecture, model training, and loss function.

Network Architecture. We design a new autoencoder-based network architecture [36] (M in Figure 3) as a watermark generator (FW-Gen), which mainly includes an encoder and a decoder, as shown in step 1 of Figure 3. The encoder converts a random Gaussian noise image ϵ into a hidden input z , and then the decoder converts z into a watermark t . Formally, we describe the network structure as follows:

$$t = M(\epsilon) = g(h(\epsilon)), \quad (10)$$

where the encoder g and the decoder h are five convolutional layers followed by ReLU layers, respectively.

Model Training. To train a benign model, we filter clean images from the dataset \tilde{D} containing watermarked images to form a dataset D_{bn} . We use common deep networks such as VGG [37] and ResNet [38] as the backbone network to train a benign model f on the dataset D_b . It is worth noting that the suspicious model \tilde{f} that the owner can access is a deep network model trained on the dataset \tilde{D} . In order to facilitate the calculation of distillation loss later, the last layer f and \tilde{f} of the model will output two probability distributions ($k = 0, 1, \dots, K - 1$):

$$p_k^T = \frac{\exp(s_k/T)}{\sum_{j=1}^K \exp(s_j/T)}, \quad p_k = \frac{\exp(s_k)}{\sum_{j=1}^K \exp(s_j)}, \quad (11)$$

where s_k is the input of the last layer, and T is the predefined temperature parameter². For any input x , we denote the

two class probability distributions of models f and \tilde{f} as $p^T(x), p(x)$ and $\tilde{p}^T(x), \tilde{p}(x)$:

$$p^T(x), p(x) = f(x), \quad \tilde{p}^T(x), \tilde{p}(x) = \tilde{f}(x). \quad (12)$$

We use the output of samples containing watermarks under the watermarked model \tilde{f} and the benign model f (classification model) as supervision signals to train FW-Gen, where the training dataset is the benign dataset $D_b = \{(x_i, y_i)\}_{i=1}^N$. In order to realize that the forged watermark and the original watermark have similar functions but different patterns, we designs two losses: distillation loss on the watermarked model and distillation loss on the benign model.

Distillation Loss. Given a benign image x , we insert the original watermark t_{ow} and the forged watermark t_{fw} into x , respectively, thus obtaining two images $x + t_{ow}$ and $x + t_{fw}$. The distillation loss [39] distills the knowledge of the original watermark t_{ow} through the benign model and the watermarked model respectively and imparts knowledge to the forged watermark t_{fw} during the model training stage. First, for any two discrete probability distributions p and q , we define the cross-entropy $\text{CE}(q, p)$ between them as:

$$\text{CE}(q, p) = - \sum_{j=1}^K q_j \log p_j. \quad (13)$$

Based on the definition of cross-entropy, we can formally describe the distillation loss on benign model f as follows (α is a weight hyper-parameter and T is the temperature parameter of the distillation model):

$$\begin{aligned} \mathcal{L}_B &= \sum_{i=1}^N \alpha T^2 \cdot \text{CE}(p^T(x_i + t_{ow}), p^T(x_i + t_{fw})) \\ &\quad + (1 - \alpha) \cdot \text{CE}(\text{one-hot}(y_i), p(x_i + t_{fw})), \end{aligned} \quad (14)$$

where the one-hot encoding function $\text{one-hot}(y_i)$ (y_i is the ground-truth label of the benign image x_i) represents the probability distribution that the probability of the class of y_i is 1 and the probability distributions of other classes are all 0. Note that x represents the benign image, while $x + t_{ow}$ and $x + t_{fw}$ represent images containing the original and forged watermark, respectively.

According to Eqn. (12), we know that $\tilde{p}^T(x)$ and $\tilde{p}(x)$ are the two probability distribution outputs of the watermarked model \tilde{f} respectively. Similarly, we can define the distillation loss on the watermarked model \tilde{f} (\tilde{T} is the temperature parameter of the distillation model):

$$\begin{aligned} \mathcal{L}_W &= \sum_{i=1}^N \alpha \tilde{T}^2 \cdot \text{CE}(\tilde{p}^T(x_i + t_{ow}), \tilde{p}^T(x_i + t_{fw})) \\ &\quad + (1 - \alpha) \cdot \text{CE}(\text{one-hot}(\tilde{y}_i), \tilde{p}(x_i + t_{fw})). \end{aligned} \quad (15)$$

Here the one-hot function uses the target label \tilde{y} instead of the ground-truth label y_i , which is different from Eqn. (14). For a benign model, regardless of whether the image contains a watermark, its predicted value should be close to the ground truth label of its image. For a watermarked model,

Finally, we optimize the parameters of FW-Gen via the following loss:

$$\mathcal{L}_{BW} = \mathcal{L}_B + \mathcal{L}_W. \quad (16)$$

²Note that p here is equivalent to p^1 in the sense of p^T .

E. Generation of Rebuttal Evidence

When the training of FW-Gen is completed, we can use FW-Gen to generate a forged watermark with the style pattern different from the original watermark. We embed the forged watermark into a benign image to obtain the forgery watermarked image. We input the benign sample x and its corresponding two images $x + t_{ow}$ and $x + t_{fw}$ containing watermarks, including the original watermark t_{ow} and the forged watermark t_{fw} , into the classification model. We verify the equivalence of their hypothesis testing results in two scenarios (Independent model and Stealing model) and two ways of using the API (probability-available and label-only).

Stealing Model Scenario (S). To test if the forged watermarks can activate abnormal behaviors of the watermarked models, we consider stealing model scenario. We modify the label of the image containing the watermark to the target label \tilde{y} to obtain the watermarked dataset, through which the watermarked model is trained. We check the output of the benign image x and the watermarked image $x + t_{ow}$ under the watermarked model f to determine whether the model used the watermarked datasets for training. If the output probability matrices are used for verification, under the paired T-test shown in Eqn. (6), rejecting the hypothesis H_0 means the usage of watermarked datasets. If only the output labels are used for verification, under the Wilcoxon test shown in Eqn. (8), rejecting the hypothesis H_0 means the usage of watermarked datasets.

Independent Model Scenario (I). Except for the stealing model scenario, in order to know if the forged watermarks are based on the original watermarks used in the protected public datasets instead of the vulnerabilities of the specific model structure, we consider independent model scenario. We use benign samples (without embedding watermarks and modifying labels) to obtain a benign dataset, and train a benign model f on it. Likewise, we check that the outputs of x and $x + t_{ow}$ under the benign model f . If the output probability vectors are used for verification, accepting the hypothesis H_0 in the paired T-test from Eqn. (6) means that the watermark t_{ow} can not cause the abnormal behaviors of benign model and the watermarked samples have the same effect with the benign samples to the benign model, which means that the abnormal behaviors are independent with the model structure, but relate with used watermarks in the protected public datasets. If only the output labels are used for verification, under the Wilcoxon test shown in Eqn. (8), accepting the hypothesis H_0 in the Wilcoxon test from Eqn. (8) means that the abnormal behaviors are independent with the model structure.

Rebuttal Evidence. Except for the p -values of the paired T-test shown in Eqn. (6) and the Wilcoxon test shown in Eqn. (8), following the configuration in [8], we additionally adopt ΔP for further evaluation. As same as T-test, we input benign samples x , samples embedded with original watermark $x + t_{ow}$, and samples embedded with forged watermark $x + t_{fw}$ to the models watermarked with original watermark t_{ow} to obtain output probability matrices P_{bn} , P_{ow} , and P_{fw} , respectively,

TABLE I
DESCRIPTION OF DATASET

Datasets	Classes	Train	Test	Total Number
CIFAR-10	10	50,000	10,000	60,000
ImageNet	200	100,000	10,000	110,000

and ΔP is defined as

$$\Delta P = \frac{1}{N} \sum_{i=1}^N (P_w(i, \tilde{y}) - P_{bn}(i, \tilde{y})), \quad (17)$$

where \tilde{y} denotes the target label, and P_w denotes one of P_{ow} and P_{fw} . Note that ΔP is not calculated in Wilcoxon test scenario since only label information can be obtained in this scenario.

Through this process, we obtain rebuttal evidence, including the p -value, ΔP , the suspicious model's output probability matrices P_{fw} and P_{bn} , the target label \tilde{y} , the predicted label y_{fw} , and the forged watermark t_{fw} .

F. Court Decision

After generating the rebuttal evidence, the attacker submits it to the court for defense. The court will make a judgment based on the evidence provided by the owner (plaintiff) and the attacker (defendant). However, due to the different watermarks provided by both parties, the attacker's rebuttal evidence can prove that the dataset used by the suspicious model is not the protected dataset released by the owner. Therefore, the court will consider the owner's evidence insufficient and rule that the accusation against the attacker is invalid.

VI. EXPERIMENTS

In this section, we evaluate the proposed FW-Gen under various conditions to answer the following research questions:

- **RQ1:** Can an attacker legally obtain the watermark information in the protected dataset?
- **RQ2:** Under various conditions, how are the performance and style of the forged watermarks generated by FW-Gen compared with the original watermarks?
- **RQ3:** How do the various loss functions in FW-Gen affect the performance of forged watermarks?

A. Experimental Setup

We will detail datasets, watermarking methods (which also serve as backdoor attack methods), and evaluation metrics employed in our experiments.

Datasets. We utilize two popular image classification datasets: CIFAR-10 and ImageNet as our benign datasets, as show in Table I, some specific details of which are described below

- **CIFAR-10 (C10)** [3] is a widely recognized open-source dataset for image classification tasks. It includes 60,000 color images of size 32×32 , divided into 10 categories, with 50,000 images for training and 10,000 for testing.
- **ImageNet (IM)** [4] is the world's largest open-source image database and the primary benchmark for evaluating image classification algorithms. It contains over 14

TABLE II

IN THE PROBABILISTIC SCENARIO, THE STATISTICAL SIGNIFICANCE COMPARISON RESULTS OF THE FORGED WATERMARK AND THE ORIGINAL WATERMARK ON CIFAR-10 (C10) AND IMAGENET (IM) BY VARIOUS BACKDOOR WATERMARKING METHODS, WHERE M AND BW REPRESENT THE CLASSIFICATION MODEL AND THE BACKDOOR WATERMARKING METHOD, RESPECTIVELY. NOTING THAT BADNETS AND BLENDED METHODS CONSIDER TWO DIFFERENT SHAPES: CROSS AND LINE. THE RED MARK INDICATES THAT THE FORGED WATERMARK SHOWS STRONGER STATISTICAL SIGNIFICANCE THAN THE ORIGINAL WATERMARK. (PROBABILITY-AVAILABLE: S : p -VALUE \downarrow , ΔP \uparrow . I : p -VALUE \uparrow , ΔP \downarrow .)

Data	M	BW Shape Metric	Badnets								Blended							
			Cross				Line				Cross				Line			
			p -value		ΔP		p -value		ΔP		p -value		ΔP		p -value		ΔP	
C10	Res	S	1.2e-173	1.1e-173	9.9e-1	9.9e-1	2.1e-107	1.8e-101	9.9e-1	9.8e-1	4.8e-164	9.5e-165	9.9e-1	9.9e-1	5.0e-54	1.4e-121	9.3e-1	9.8e-1
		I	1	1	7.9e-4	7.9e-4	1	1	-3.6e-4	-3.6e-4	1	1	6.2e-1	6.2e-1	1	1	-2.3e-4	-2.3e-4
	VGG	S	7.3e-144	1.1e-143	9.9e-1	9.9e-1	4.6e-92	3.2e-75	9.8e-1	9.7e-1	6.8e-241	3.7e-241	9.9e-1	9.9e-1	7.7e-59	1.5e-96	9.4e-1	9.7e-1
		I	1	1	5.4e-5	5.4e-5	1	1	-5.8e-5	-5.8e-5	1	1	1.8e-4	1.8e-4	1	1	-1.9e-4	-1.9e-4
IM	Res	S	6.2e-180	1.4e-177	9.9e-1	9.9e-1	8.6e-59	4.3e-63	9.4e-1	9.3e-1	1.6e-30	1.3e-65	7.6e-1	8.8e-1	2.2e-18	2.4e-25	6.5e-1	6.5e-1
		I	1	1	8.2e-6	8.2e-6	1	1	5.2e-6	5.2e-6	1	1	5.0e-6	5.0e-6	1	1	-2.2e-7	-2.2e-7
	VGG	S	2.2e-181	2.2e-181	9.9e-1	9.9e-1	9.3e-62	3.8e-112	9.5e-1	9.7e-1	8.9e-49	2.1e-77	8.8e-1	9.5e-1	1.2e-31	7.6e-72	8.1e-1	9.5e-1
		I	1	1	-1.9e-7	-1.9e-7	1	1	2.7e-6	2.7e-6	1	1	6.7e-8	6.7e-8	1	1	2.7e-6	2.7e-6

Data	M	BW Metric	l_0 inv				Nature				Trojan_sq				Trojan_wm			
			p -value		ΔP		p -value		ΔP		p -value		ΔP		p -value		ΔP	
			C10	Res	S	7.7e-215	4.1e-214	9.9e-1	9.9e-1	2.7e-146	2.3e-146	9.9e-1	9.9e-1	2.0e-247	2.2e-247	9.9e-1	9.9e-1	4.6e-192
I	1	1			2.5e-4	2.5e-4	1	1	2.6e-2	2.6e-2	1	1	4.1e-3	4.1e-3	1	1	1.7e-2	1.7e-2
VGG	S	3.7e-184		8.8e-115	2.5e-4	2.5e-4	3.5e-256	3.8e-111	9.9e-1	9.8e-1	1.6e-227	1.5e-227	9.9e-1	9.9e-1	1.5e-124	1.5e-124	9.9e-1	9.9e-1
	I	1		1	-5.3e-3	-5.3e-3	1	1	5.2e-2	5.2e-2	1	1	6.4e-2	6.4e-2	1	1	8.6e-2	8.6e-2
IM	Res	S	1.0e-240	1.3e-241	9.9e-1	9.9e-1	1.0e-224	4.5e-181	9.9e-1	9.9e-1	6.1e-199	9.9e-131	9.9e-1	9.8e-1	2.9e-236	2.3e-236	9.9e-1	9.9e-1
		I	1	1	9.9e-5	9.9e-5	1	1	1.6e-3	1.6e-3	1	1	1.0e-3	1.0e-3	1	1	2.1e-2	2.1e-2
	VGG	S	0	0	1	1	0	0	1	1	0	0	1	1	0	0	1	1
		I	1	1	3.6e-6	3.6e-6	1	1	4.5e-5	4.5e-5	1	1	2.6e-4	2.6e-4	1	1	9.8e-3	9.8e-3

million images across 20,000 categories. In our work, we randomly select a subset of 100,000 images from 200 classes, with 500 images per class for the training set. For the testing set, we select 10,000 images, with 50 images per class.

Baseline. We employ classical backdoor attack methods as benchmarks for the original watermarks to evaluate the efficacy of our method. Below is a brief description of the backdoor attack methods used in the experiments.

- **Badnets [21]:** A backdoor attack method using pixel blocks as triggers.
- **Blended [22]:** A backdoor attack method mixing natural images and triggers.
- l_0 **inv [23]:** A backdoor attack method using sparse triggers based on l_0 paradigms.
- **Nature [22]:** A backdoor attack method using natural images embedded with semantic information as triggers.
- **Trojan square (Trojan_sq) [24]:** A backdoor attack method using a specific shape as a trigger.
- **Trojan watermark (Trojan_wm) [24]:** A backdoor attack method using a digital watermark as a trigger.

Parameter Settings. We use two classic classification models, namely VGG-19 (VGG) [37] and ResNet-18 (Res) [38], and set the poisoning rate to $\gamma = 0.1$. At the same time, the target label \tilde{y} of the watermarked image is specified as ‘0’. For the Blended method, we adjust the transparency to $\rho \in [0, 0.2]$. We set the temperature parameter of the distillation loss to 500 in the Cross condition and to 800 in other conditions. In the training stage, we configure the learning rate (lr) to 0.008, 500 iterations, batch size to 32, and then use the AdamW optimizer for optimization.

B. Evaluation Metrics

In order to effectively verify the effectiveness of our method, we verify the equivalence and difference of metrics on the forged watermark and the original watermark from three aspects: hypothesis test, classification performance, and image quality.

Metrics for Hypothesis Test. We employ p -value (with an additional ΔP for the case of probability-available) [8], [9] to test whether the classification model is trained with the protected dataset, where the usage scenarios include the independent model and the stealing model.

Metrics for Classification Performance. We use an watermark dataset that contains both benign and watermarked images. We separately count the accuracy on the benign image set and the watermarked image set in the test set, that is, the benign accuracy (BA) and the watermark success rate (WSR) [8], which respectively represent the proportion of successfully predicted images in the benign image set and the watermarked image set. To visually compare the attack effectiveness of the original watermark with the forged watermark, we apply the watermark success rates produced by these two types of watermarks, *i.e.*, the original watermark success rate (OWSR) and the forged watermark success rate (FWSR).

Metrics for Image Quality. Our goal is to create fake watermarks that retain the functionality of the original watermark but exhibit a unique style. To this end, we analyzed the pattern differences between the two watermarks, employing three widely recognized image processing metrics to evaluate image quality so that we can visually observe the differences, including: peak signal-to-noise ratio (PSNR) [40], mean squared error (MSE) and structural similarity index measurement (SSIM) [41].

C. Watermark Detection

To answer **RQ1**, we employ an effective watermark detection algorithm, *i.e.*, an attacker can legally detect the watermark on the protected public dataset, to verify that backdoor watermark data can be obtained from a given dataset in a black-box manner. We use a frequency-domain-based detection method³ to distinguish backdoor watermark data from benign data in the dataset, and use backdoor watermark

³<https://github.com/YiZeng623/frequency-backdoor>

TABLE III
RECOGNITION ACCURACY (%) OF THE BACKDOOR WATERMARKING METHOD ON THE WATERMARKED IMAGE DATASET ON CIFAR-10 (C10).

Data	Badnets	Blended	l_0 inv	Nature	Trojan_sq	Trojan_wm
C10	90.2	99.1	100	99.4	99.8	99.9

TABLE IV

IN THE LABEL-ONLY SCENARIO, THE STATISTICAL SIGNIFICANCE COMPARISON RESULTS OF THE FORGED WATERMARK AND THE ORIGINAL WATERMARK ON CIFAR-10 (C10) AND IMAGENET (IM) BY VARIOUS BACKDOOR WATERMARKING METHODS. THE RED MARK INDICATES THAT THE FORGED WATERMARK SHOWS STRONGER STATISTICAL SIGNIFICANCE THAN THE ORIGINAL WATERMARK. (LABEL-ONLY: S : p -VALUE ↓, I : p -VALUE ↑.)

Data	M	Badnets										
		BW		Cross			Line			Blended		
		Shape	Metric	p -value	p -value	p -value	p -value	p -value	p -value	p -value		
C10	Res	S	0	0	0	1.5e-2	0	0	0	0	7.4e-3	0
		I	1	1	1	1	1	1	1	1	1	1
	VGG	S	0	0	1.5e-3	3.0e-3	0	0	0	0	5.5e-3	0
		I	1	1	1	1	1	1	1	1	1	1
IM	Res	S	0	0	5.5e-3	5.5e-3	9.9e-3	7.4e-3	1	1	1	1
		I	1	1	1	1	1	1	1	1	1	1
	VGG	S	0	0	5.5e-3	0	9.3e-3	3.0e-3	9.9e-3	3.0e-3	1	1
		I	1	1	1	1	1	1	1	1	1	1

Data	M	BW		l_0 inv	Nature	Trojan_sq	Trojan_wm
		Metric	p -value	p -value	p -value	p -value	p -value
C10	Res	S	0	0	0	0	0
		I	1	1	1	1	1
	VGG	S	0	1.5e-3	0	0	0
		I	1	1	1	1	1
IM	Res	S	0	0	0	0	0
		I	1	1	1	1	1
	VGG	S	0	0	0	0	0
		I	1	1	1	1	1

data detection rate (BWDR) as the evaluation metric [28]. The higher the BWDR, the more effective the detection result.

Table III shows the experimental results of six backdoor watermark methods on the CIFAR-10 dataset. It can be observed that for datasets with different backdoor watermarks, except for Badnets, the BWDR is close to 100%. This shows that an attacker can effectively obtain backdoor watermark data from almost any dataset in a black-box manner.

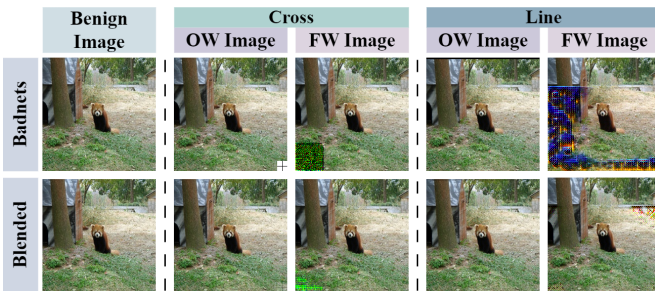


Fig. 4. Examples of benign, original watermarked (OW), and forged watermarked (FW) images using the Badnets and Blended backdoor watermark attack methods, where the crosses and lines represent different styles of the original watermark, respectively.

D. Comparison between forged and original watermarks

To demonstrate the consistency of forged watermarks and original watermarks in copyright verification in **RQ2**, we adopt various backdoor watermarking methods in two types of APIs

(probability available and label-only) and two scenarios (independent model and stolen model) to verify the equivalence between the original watermark and the forged watermark, as shown in Figure 4. For BadNet and Blended methods, we follow the protocol in [42] to embed **Cross** (the small block in the lower right corner) and **Line** (the thick black line at the top) into the image to obtain the watermarked image⁴. For other backdoor watermarking methods, we conduct experiments according to the description in the original literature [22]–[24]. **Consistency of Hypothesis Testing.** For the case where the classification model outputs probability (i.e., probability available API), we perform T-tests on the original watermark dataset and the forged watermark dataset respectively, and determine the dataset infringement based on the significance level of the statistical results (Table II). Similarly, when the classification model only outputs labels (label-only API), the Wilcoxon signed rank test is performed on the original watermark dataset and the forged watermark dataset to obtain the p -values, as shown in Table IV.

In the stealing model scenario, we use a one-sided T-test. When ΔP is larger and the p -value is smaller, the probability of rejecting the null hypothesis is greater. Unlike the stealing model, for the independent model scenario, when we use a one-sided T-test, the smaller the ΔP value and the larger the corresponding p -value, the greater the probability of accepting the null hypothesis.

According to the theory of hypothesis testing, we can draw the following conclusions from the results of Tables (Table II and IV)

- The p -value in the stealing model or the $1-p$ value in the independent model is much smaller than the significance level of 0.05 usually set in statistics.
- In the probability available scenario, both the original watermark and the forged watermark can accurately determine with high confidence that the dataset has been stolen. Here, the p -value in the theft model scenario is close to 0, $\Delta P \gg 0$, while in the independent model scenario, the p -value $\gg 0.05$, ΔP is close to 0.
- In the probability available scenario, whether in the stealing model scenario or the independent model scenario, the p -value and ΔP of the forged watermark are the same as or even higher than the original watermark, as shown in the red marks in Table II. This shows that in copyright verification, the forged watermark shows at least the same or even stronger statistical significance as the original watermark.

Comparison of Classification Performance. We analyze the BA (benign accuracy) and WSR (watermark success rate) of the two watermarks. From the results in Table V, we can see that compared with the performance of the watermarked model on the benign image test set, the performance on the watermarked image test set usually decreases by less than 1%, and in some cases it is slightly improved, which further proves that watermarking technology does not hinder the use of normal datasets. It is worth noting that the success rate of the forged watermark (FWSR) is very close to or exceeds the

⁴<https://github.com/THUYimingLi/DVBW>

TABLE V

COMPARISON OF THE BENIGN ACCURACY (BA) (%), THE SUCCESS RATE OF THE ORIGINAL WATERMARK (OWSR) (%), AND THE SUCCESS RATE OF THE FORGED WATERMARK (FWSR) (%) OF THE BACKDOOR WATERMARKING METHOD ON THE CIFAR-10 (C10) AND IMAGENET (IM) DATASETS, WHERE RESNET-18 (RES) AND VGG-19 (VGG) ARE TWO DIFFERENT SUSPICIOUS MODELS, AND NONE REPRESENTS THAT THE MODEL RUNS ON THE BENIGN DATASET WITHOUT ADDING A WATERMARK.

Data	BW	None	Badnets						Blended					
	Shape		Cross				Line		Cross			Line		
	Metric		BA	BA	OWSR	FWSR	BA	OWSR	FWSR	BA	OWSR	FWSR	BA	OWSR
C10	Res	91.4	91.9	100	100	91.7	99.8	99.9	91.6	100	100	91.3	93.9	99.0
	VGG	91.7	91.6	100	100	91.6	99.6	98.4	91.2	99.8	100	90.2	93.1	97.0
IM	Res	87.0	86.7	99.8	99.8	86.0	96.4	95.6	86.3	90.9	95.3	85.4	81.0	86.9
	VGG	90.6	89.4	100	99.9	89.8	97.7	98.4	89.5	95.6	98.8	89.7	89.3	94.4

Data	BW	None	l_0 inv		Nature			Trojan_sq			Trojan_wm			
	Metric		BA	BA	OWSR	FWSR	BA	OWSR	FWSR	BA	OWSR	FWSR		
	C10		Res	93.5	92.9	100	100	93.5	100	100	92.6	99.8	100	93.2
VGG		93.0	92.9	100	99.2	91.7	100	98.9	92.2	99.9	100	92.8	100	100
IM	Res	88.2	89.8	100	100	89.7	99.8	99.4	89.8	100	99.6	89.5	100	99.7
	VGG	91.2	92.7	100	100	92.8	100	100	93.4	100	100	93.1	100	100

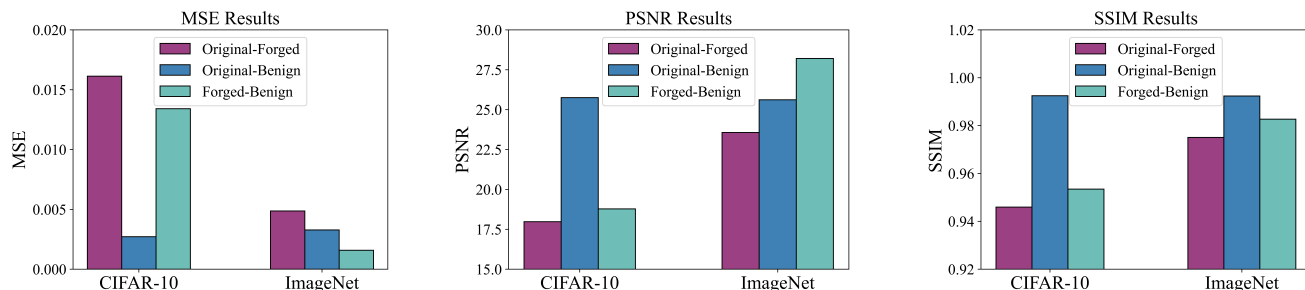


Fig. 5. Comparisons of PSNR, SSIM, and MSE metrics using the Badnets method and ResNet-18 models trained on the CIFAR-10 and ImageNet datasets as target models, with Original-Forged, Original-Benign, and Forged-Benign representing the comparative pairs of original watermarked images and forged watermarked images, original watermarked images and benign images, and forged watermarked images and benign images, respectively.

success rate of the original watermark (OWSR). For example, on the Blended Line watermark dataset, the success rate of the forged watermark is a significant improvement over the original watermark (86.9% vs. 81.0%). These results highlight the effectiveness of the forged watermark in simulating the original watermark function.

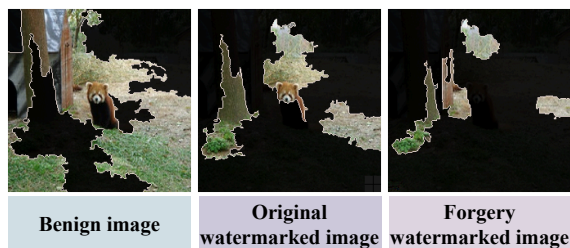


Fig. 6. LIME provides diagnostic interpretation of images with and without different watermarks, where regions contributing to the watermark classification are explicitly marked.

Differences between Original and Forged Watermarks.

To quantitatively evaluate the visual difference between the original and forged watermarks, we used three main image quality metrics: PSNR, SSIM, and MSE. Generally, lower PSNR and SSIM values indicate larger differences, while

larger MSE indicates larger differences between the pixels of the two images. We quantitatively analyzed the differences between the benign, original, and forged watermarked images, as shown in Figure 5, which shows that there are significant differences between the original and forged watermarked images. In addition, the visualization results shown in Figure 6 also clearly demonstrate the obvious differences in style between the original and forged watermarks.

Furthermore, we employ Locally Interpretable Model-Agnostic Explanations (LIME) [43] to explain the differences between the original and forged watermarks and evaluate the effectiveness of the attack. Figure 6 illustrates how LIME identifies regions that affect the watermarked model’s predictions. When analyzing benign images, the model focuses on the object itself. However, for watermarked images, the focus clearly shifts to the peripheral regions. Notably, the focus regions associated with the original watermark are significantly different from those associated with the forged watermark.

E. Ablation Study on Losses

To answer the impact of the loss function submitted in **RQ3** on FW-Gen, we conducted ablation experiments from two perspectives: hypothesis testing and classification.

TABLE VI

IN THE PROBABILITY AVAILABLE SCENARIO, THE IMPACT OF LOSS FUNCTIONS \mathcal{L}_W , \mathcal{L}_B AND \mathcal{L}_{BW} ON DIFFERENT FORGERY WATERMARKING METHODS ON THE DATASETS CIFAR-10 (C10) AND IMAGENET (IM), WHERE WE ALSO CONSIDER DIFFERENT SUSPICIOUS MODELS RES AND VGG.

Data	M	BW Shape Metric	Badnets											
			Cross			Line			Line					
			p -value ($\mathcal{L}_W \mathcal{L}_B \mathcal{L}_{WB}$)	ΔP ($\mathcal{L}_W \mathcal{L}_B \mathcal{L}_{WB}$)	p -value ($\mathcal{L}_W \mathcal{L}_B \mathcal{L}_{WB}$)	ΔP ($\mathcal{L}_W \mathcal{L}_B \mathcal{L}_{WB}$)	p -value ($\mathcal{L}_W \mathcal{L}_B \mathcal{L}_{WB}$)	ΔP ($\mathcal{L}_W \mathcal{L}_B \mathcal{L}_{WB}$)						
C10	Res	S	2.3e-172	1	1.1e-173	9.9e-1	2.9e-4	9.9e-1	1.6e-69	1	1.8e-101	8.8e-1	-3.4e-4	9.8e-1
		I	1	1	1	7.9e-4	7.9e-4	7.9e-4	1	1	1	-3.6e-4	-3.6e-4	-3.6e-4
	VGG	S	7.8e-140	1	1.1e-143	1.7e-1	-2.7e-4	9.9e-1	8.6e-205	1	3.2e-75	9.9e-1	-3.1e-4	9.7e-1
		I	1	1	1	5.4e-5	5.4e-5	5.4e-5	1	1	1	-5.8e-5	-5.8e-5	-5.8e-5
IM	Res	S	9.0e-169	1	1.4e-177	9.9e-1	-1.2e-5	9.9e-1	1.8e-118	1	4.3e-63	9.8e-1	-2.2e-4	9.3e-1
		I	1	1	1	8.2e-6	8.2e-6	8.2e-6	1	1	1	5.2e-6	5.2e-6	5.2e-6
	VGG	S	1.8e-181	1	2.2e-181	9.9e-1	-3.3e-4	9.9e-1	2.3e-300	1	3.8e-112	9.9e-1	-2.1e-6	9.7e-1
		I	1	1	1	-1.9e-7	-1.9e-7	-1.9e-7	1	1	1	2.7e-6	2.7e-6	2.7e-6

TABLE VII

IN THE LABEL-ONLY SCENARIO, ABLATION STUDY OF LOSS FUNCTIONS \mathcal{L}_W , \mathcal{L}_B AND \mathcal{L}_{BW} ON THE DATASETS CIFAR-10 (C10) AND IMAGENET (IM).

Data	M	BW Shape Metric	Badnets						Blended					
			Cross			Line			Cross			Line		
			p -value ($\mathcal{L}_W \mathcal{L}_B \mathcal{L}_{WB}$)	ΔP ($\mathcal{L}_W \mathcal{L}_B \mathcal{L}_{WB}$)	p -value ($\mathcal{L}_W \mathcal{L}_B \mathcal{L}_{WB}$)	ΔP ($\mathcal{L}_W \mathcal{L}_B \mathcal{L}_{WB}$)	p -value ($\mathcal{L}_W \mathcal{L}_B \mathcal{L}_{WB}$)	ΔP ($\mathcal{L}_W \mathcal{L}_B \mathcal{L}_{WB}$)						
C10	Res	S	1.3e-164	1	9.5e-165	9.9e-1	2.5e-3	9.9e-1	1.0e-161	1	1.4e-121	9.9e-1	4.7e-3	9.8e-1
		I	1	1	1	6.2e-5	6.2e-5	6.2e-5	1	1	1	-2.3e-4	-2.3e-4	-2.3e-4
	VGG	S	2.7e-241	1	3.7e-241	9.9e-1	1.2e-4	9.9e-1	3.9e-68	1	1.5e-96	4.1e-1	6.3e-3	9.7e-1
		I	1	1	1	1.8e-4	1.8e-4	1.8e-4	1	1	1	-1.9e-4	-1.9e-4	-1.9e-4
IM	Res	S	1.2e-52	1	1.35e-65	8.7e-1	2.3e-5	8.8e-1	8.1e-48	1	2.4e-25	7.8e-1	-1.9e-4	6.5e-1
		I	1	1	1	5.0e-6	5.0e-6	5.0e-6	1	1	1	-2.4e-7	-2.4e-7	-2.2e-7
	VGG	S	2.3e-125	1	2.1e-77	9.7e-1	-1.1e-4	9.5e-1	1.7e-177	1	7.6e-72	9.8e-1	-9.6e-6	9.5e-1
		I	1	1	1	6.2e-8	6.2e-8	6.7e-8	1	1	1	2.7e-6	2.7e-6	2.7e-6

TABLE VIII

ABLATION STUDY OF THE LOSS FUNCTION (\mathcal{L}_B , \mathcal{L}_W , \mathcal{L}_{BW}) ON THE FORGED WATERMARK SUCCESS RATE (FWSR) ON DIFFERENT DATASETS INCLUDING CIFAR-10 (C10) AND IMAGENET (IM) AND DIFFERENT BACKDOOR WATERMARKING METHODS (BADNETS AND BLENDED).

Data	BW Shape Metric	Badnets						Blended					
		Cross			Line			Cross			Line		
		FWSR ($\mathcal{L}_W \mathcal{L}_B \mathcal{L}_{WB}$)	FWSR ($\mathcal{L}_W \mathcal{L}_B \mathcal{L}_{WB}$)	FWSR ($\mathcal{L}_W \mathcal{L}_B \mathcal{L}_{WB}$)	FWSR ($\mathcal{L}_W \mathcal{L}_B \mathcal{L}_{WB}$)	FWSR ($\mathcal{L}_W \mathcal{L}_B \mathcal{L}_{WB}$)	FWSR ($\mathcal{L}_W \mathcal{L}_B \mathcal{L}_{WB}$)						
C10	Res	100	1.4	100	98.3	0.9	99.9	100	0.9	100	100	1.1	99.0
	VGG	16.5	1.3	100	100	1.2	98.4	100	1.3	100	45.3	1.3	97.0
IM	Res	99.5	0.2	99.8	100	0.4	95.6	96.1	0.2	95.3	95.5	2.0	86.9
	VGG	100	0.1	99.9	100	0.1	98.4	99.5	0.1	98.8	100	0.1	94.4

Hypothesis Testing. We conduct ablation experiments on the loss function of FW-Gen using Badnets and Blended methods to evaluate the impact of two different loss pairs on the hypothesis testing results, as shown in Tables VI, and VII. We find that **for hypothesis testing, \mathcal{L}_W loss is more important than \mathcal{L}_B** , where the p -value of \mathcal{L}_B is always equal to 1, which is consistent with our intuition. Since the watermarked images (including original watermarks and forged watermarks) and benign images perform similarly on the benign model, the loss \mathcal{L}_B has little impact on the benign model.

Classification. We further analyze the impact of the two

loss functions on the classification performance, as shown in Table VIII. We find that although the distillation loss \mathcal{L}_W on the watermarked model plays an important role in most cases, there are two exceptions, as shown in the red and blue fonts in Table VIII. On the VGG-19 model, the success rate of watermark attack using only loss \mathcal{L}_W is only 16.5% and 45.3%, while after adding loss \mathcal{L}_B , the success rate of watermark attack is greatly improved, reaching 100% and 97% respectively. This indicates that **\mathcal{L}_B also plays an important role in improving WSR compared with \mathcal{L}_W .**

VII. CONCLUSION

We improve the practicality of the backdoor watermarking process by introducing a third-party judicial institution (such as a court), and mainly study the reliability of the statistical hypothesis testing method for public dataset ownership verification under the background of backdoor watermarking. We propose a forged watermark generator (FW-Gen) based on the idea of distillation learning. The original watermarked image and the forged watermarked image are respectively input into the classification model (benign model or watermarked model) to obtain two probability distributions. Here we define two distillation losses to drive the algorithm to optimize only the parameters of FW-Gen. A large number of experiments show that the hypothesis test of forged watermarks and original watermarks in dataset copyright verification has the same statistical significance from multiple perspectives, such as various backdoor watermarks, classification models (VGG-19 or Resnet), model output types (probability available or only labels), application scenarios (independent models or stolen models), and so on. The results show that the forged watermarks and the original watermarks have the same statistical significance in the hypothesis testing of dataset copyright verification, and have similar classification performance on the model.

Although our main motivation is to study the reliability and security challenges of copyright verification of datasets from the perspective of forgery attacks, the insights gained from the forgery process may provide valuable guidance for improving the reliability of copyright verification. First, the target label is crucial in the forgery process, so the data owner can mislead the attacker by specifying multiple target labels. Second, since the generation of forged images requires filtering the backdoor watermark data, developing more invisible and undetected backdoor watermarks can complicate the attacker's efforts to identify the backdoor watermark data. We hope that our work can provide new thinking and research directions for the security issues of backdoor watermarks in the future.

REFERENCES

- [1] B. Mann, N. Ryder, M. Subbiah, J. Kaplan, P. Dhariwal, A. Neelakantan, P. Shyam, G. Sastry, A. Askell, S. Agarwal *et al.*, "Language models are few-shot learners," *arXiv:2005.14165*, vol. 1, 2020.
- [2] H. Touvron, T. Lavril, G. Izacard, X. Martinet, M.-A. Lachaux, T. Lacroix, B. Rozière, N. Goyal, E. Hambro, F. Azhar *et al.*, "Llama: Open and efficient foundation language models," *arXiv:2302.13971*, 2023.
- [3] A. Krizhevsky, G. Hinton *et al.*, "Learning multiple layers of features from tiny images," 2009.
- [4] J. Deng, W. Dong, R. Socher, L.-J. Li, K. Li, and L. Fei-Fei, "Imagenet: A large-scale hierarchical image database," in *Computer Vision and Pattern Recognition*, 2009, pp. 248–255.
- [5] M. Everingham, L. Van Gool, C. K. Williams, J. Winn, and A. Zisserman, "The pascal visual object classes (voc) challenge," *International Journal of Computer Vision*, vol. 88, pp. 303–338, 2010.
- [6] T.-Y. Lin, M. Maire, S. Belongie, J. Hays, P. Perona, D. Ramanan, P. Dollár, and C. L. Zitnick, "Microsoft coco: Common objects in context," in *European Conference on Computer Vision*, 2014, pp. 740–755.
- [7] C. Sakaridis, D. Dai, and L. Van Gool, "Semantic foggy scene understanding with synthetic data," *International Journal of Computer Vision*, vol. 126, pp. 973–992, 2018.
- [8] Y. Li, M. Zhu, X. Yang, Y. Jiang, T. Wei, and S.-T. Xia, "Black-box dataset ownership verification via backdoor watermarking," *IEEE Transactions on Information Forensics and Security*, 2023.
- [9] Y. Li, Y. Bai, Y. Jiang, Y. Yang, S.-T. Xia, and B. Li, "Untargeted backdoor watermark: Towards harmless and stealthy dataset copyright protection," *Advances in Neural Information Processing Systems*, vol. 35, pp. 13 238–13 250, 2022.
- [10] R. Tang, Q. Feng, N. Liu, F. Yang, and X. Hu, "Did you train on my dataset? towards public dataset protection with cleanlabel backdoor watermarking," *ACM SIGKDD Explorations Newsletter*, vol. 25, no. 1, pp. 43–53, 2023.
- [11] J. Guo, Y. Li, L. Wang, S.-T. Xia, H. Huang, C. Liu, and B. Li, "Domain watermark: Effective and harmless dataset copyright protection is closed at hand," *Advances in Neural Information Processing Systems*, vol. 36, 2024.
- [12] L. Wang, S. Xu, R. Xu, X. Wang, and Q. Zhu, "Non-transferable learning: A new approach for model ownership verification and applicability authorization," in *International Conference on Learning Representation*, 2022.
- [13] G. A. Kaissis, M. R. Makowski, D. Rückert, and R. F. Braren, "Secure, privacy-preserving and federated machine learning in medical imaging," *Nature Machine Intelligence*, vol. 2, no. 6, pp. 305–311, 2020.
- [14] Y. Miao, Z. Liu, H. Li, K.-K. R. Choo, and R. H. Deng, "Privacy-preserving byzantine-robust federated learning via blockchain systems," *IEEE Transactions on Information Forensics and Security*, vol. 17, pp. 2848–2861, 2022.
- [15] J. Li, Q. Yu, and Y. Zhang, "Hierarchical attribute based encryption with continuous leakage-resilience," *Information Sciences*, vol. 484, pp. 113–134, 2019.
- [16] H. Deng, Z. Qin, Q. Wu, Z. Guan, R. H. Deng, Y. Wang, and Y. Zhou, "Identity-based encryption transformation for flexible sharing of encrypted data in public cloud," *IEEE Transactions on Information Forensics and Security*, vol. 15, pp. 3168–3180, 2020.
- [17] R. Wang, F. Juefei-Xu, M. Luo, Y. Liu, and L. Wang, "Faketagger: Robust safeguards against deepfake dissemination via provenance tracking," in *ACM International Conference on Multimedia*, 2021, pp. 3546–3555.
- [18] Z. Guan, J. Jing, X. Deng, M. Xu, L. Jiang, Z. Zhang, and Y. Li, "Deepmih: Deep invertible network for multiple image hiding," *IEEE Transactions on Pattern Analysis and Machine Intelligence*, vol. 45, no. 1, pp. 372–390, 2022.
- [19] S. Wang, J. Zhou, J. K. Liu, J. Yu, J. Chen, and W. Xie, "An efficient file hierarchy attribute-based encryption scheme in cloud computing," *IEEE Transactions on Information Forensics and Security*, vol. 11, no. 6, pp. 1265–1277, 2016.
- [20] S. Haddad, G. Coatrieux, A. Moreau-Gaudry, and M. Cozic, "Joint watermarking-encryption-jpeg-ls for medical image reliability control in encrypted and compressed domains," *IEEE Transactions on Information Forensics and Security*, vol. 15, pp. 2556–2569, 2020.
- [21] T. Gu, B. Dolan-Gavitt, and S. Garg, "Badnets: Identifying vulnerabilities in the machine learning model supply chain," *arXiv preprint arXiv:1708.06733*, 2017.
- [22] X. Chen, C. Liu, B. Li, K. Lu, and D. Song, "Targeted backdoor attacks on deep learning systems using data poisoning," *arXiv preprint arXiv:1712.05526*, 2017.
- [23] S. Li, M. Xue, B. Z. H. Zhao, H. Zhu, and X. Zhang, "Invisible backdoor attacks on deep neural networks via steganography and regularization," *IEEE Transactions on Dependable and Secure Computing*, vol. 18, no. 5, pp. 2088–2105, 2020.
- [24] Y. Liu, S. Ma, Y. Aafer, W.-C. Lee, J. Zhai, W. Wang, and X. Zhang, "Trojaning attack on neural networks," in *Network and Distributed System Security*, 2018.
- [25] Y. Gao, C. Xu, D. Wang, S. Chen, D. C. Ranasinghe, and S. Nepal, "Strip: A defence against trojan attacks on deep neural networks," in *Computer Security Applications*, 2019, pp. 113–125.
- [26] N. Peri, N. Gupta, W. R. Huang, L. Fowl, C. Zhu, S. Feizi, T. Goldstein, and J. P. Dickerson, "Deep k-nn defense against clean-label data poisoning attacks," in *European Conference on Computer Vision Workshop*, 2020, pp. 55–70.
- [27] B. Tran, J. Li, and A. Madry, "Spectral signatures in backdoor attacks," *Advances in Neural Information Processing Systems*, vol. 31, 2018.
- [28] Y. Zeng, W. Park, Z. M. Mao, and R. Jia, "Rethinking the backdoor attacks' triggers: A frequency perspective," in *International Conference on Computer Vision*, 2021, pp. 16 473–16 481.
- [29] K. Doan, Y. Lao, and P. Li, "Backdoor attack with imperceptible input and latent modification," *Advances in Neural Information Processing Systems*, vol. 34, pp. 18 944–18 957, 2021.
- [30] Z. Zhao, X. Chen, Y. Xuan, Y. Dong, D. Wang, and K. Liang, "Defeat: Deep hidden feature backdoor attacks by imperceptible perturbation and latent representation constraints," in *Computer Vision and Pattern Recognition*, 2022, pp. 15 213–15 222.

- [31] A. Bansal, P.-y. Chiang, M. J. Curry, R. Jain, C. Wington, V. Manjunatha, J. P. Dickerson, and T. Goldstein, "Certified neural network watermark with randomized smoothing," in *International Conference on Machine Learning*, 2022, pp. 1450–1465.
- [32] Y. Wang, Z. Ding, Y. Xiao, D. Kifer, and D. Zhang, "Dpgen: Automated program synthesis for differential privacy," in *ACM Conference on Computer and Communications Security*, 2021, pp. 393–411.
- [33] M. Du, X. Yue, S. S. Chow, T. Wang, C. Huang, and H. Sun, "Dp-forward: Fine-tuning and inference on language models with differential privacy in forward pass," in *ACM Conference on Computer and Communications Security*, 2023, pp. 2665–2679.
- [34] R. L. Wasserstein and N. A. Lazar, "The asa statement on p-values: context, process, and purpose," *The American Statistician*, vol. 70, no. 2, pp. 129–133, 2016.
- [35] I. J. Goodfellow, J. Shlens, and C. Szegedy, "Explaining and harnessing adversarial examples," *arXiv preprint arXiv:1412.6572*, 2014.
- [36] W. H. L. Pinaya, S. Vieira, R. Garcia-Dias, and A. Mechelli, "Autoencoders," in *Machine learning*, 2020, pp. 193–208.
- [37] K. Simonyan and A. Zisserman, "Very deep convolutional networks for large-scale image recognition," *arXiv:1409.1556*, 2014.
- [38] K. He, X. Zhang, S. Ren, and J. Sun, "Deep residual learning for image recognition," in *Computer Vision and Pattern Recognition*, 2016, pp. 770–778.
- [39] G. Hinton, O. Vinyals, and J. Dean, "Distilling the knowledge in a neural network," *arXiv preprint arXiv:1503.02531*, 2015.
- [40] T. Wang, X. Yang, K. Xu, S. Chen, Q. Zhang, and R. W. Lau, "Spatial attentive single-image deraining with a high quality real rain dataset," in *Computer Vision and Pattern Recognition*, 2019, pp. 12 270–12 279.
- [41] Z. Wang, A. C. Bovik, H. R. Sheikh, and E. P. Simoncelli, "Image quality assessment: from error visibility to structural similarity," *IEEE Transactions on Image Processing*, vol. 13, no. 4, pp. 600–612, 2004.
- [42] Y. Li, M. Ya, Y. Bai, Y. Jiang, and S.-T. Xia, "BackdoorBox: A python toolbox for backdoor learning," in *International Conference on Learning Representation Workshop*, 2023.
- [43] M. T. Ribeiro, S. Singh, and C. Guestrin, "“why should i trust you?” explaining the predictions of any classifier," in *ACM KDD*, 2016, pp. 1135–1144.



Zhiying Li received the B.Sc degree from College of Cyber Security Jinan University, Guangzhou, China, in 2023. He is currently an Ph.D. with the College of Information Science and Technology / College of Cyber Security, Jinan University, China. His research interests mainly focus on AI security, privacy protection, and low-level image analysis.



Zhi Liu is currently pursuing a Bachelor's degree in Cyber Security at Jinan University, Guangzhou, China. His research interests mainly focus on AI security, including backdoor attacks, adversarial attacks, and privacy protection.



Dong-Jie Liu received her Ph.D. degree from Computer Network Information Center, Chinese Academy of Sciences, University of Chinese Academy of Sciences, Beijing, China. She now works in College of Cyber Security, Jinan University, Guangzhou. Her research interests include Web security, machine learning and blockchain. She has published papers including international authoritative journals and conferences such as Expert Systems With Applications, Computers and Security and ICT Express. She also serves as the program chair of

ACM ICEA'2023 & 2021 and technical committee member of ACM IECC'2020.



Sheng-Da Zhuo (Student Member, IEEE) received the MS degree in computer science and technology from Guangzhou University, Guangzhou, China, in 2023. He is currently working toward the PhD degree in cyberspace security with Jinan University, Guangzhou, China. His research interests include machine learning, recommendation systems, and data mining.



retrieval on the web, and web search.

Guanggang Geng received the Ph.D. degree from the State Key Laboratory of Management and Control for Complex Systems, Institute of Automation, Chinese Academy of Sciences, Beijing, China. He was with the Computer Network Information Center, Chinese Academy of Sciences, Beijing. He was with the China Internet Network Information Center, Beijing, from 2016 to 2020. He is currently a Professor with the College of Cyber Security, Jinan University, Guangzhou. His current research interests include machine learning, anti-fraud, adversarial information



retrieval on the web, and web search.

Jian Weng (Senior Member, IEEE) received the Ph.D. degree in computer science and engineering from Shanghai Jiao Tong University in 2008. From 2008 to 2010, he held a postdoctoral position with the School of Information Systems, Singapore Management University. He is currently a Professor and the Vice President of Jinan University. He has published more than 100 papers in cryptography and security conferences and journals, such as Cryptography, EUROCRYPT, ASIACRYPT, ACM CCS, and USENIX Security. His research interests include cryptography, data security, and blockchain. He won the Innovation Award from Chinese Association for Cryptologic Research in 2015 and the National Science Fund for Distinguished Young Scholars in 2018. He served as the PC co-chair or a PC member for more than 50 international conferences.



National Crypto-Math Challenge of China. He was in the organizing committee of Inscript 2020. His research interests include lattice codes, wireless communications, and information security.

Shanxiang Lyu received the BS and MS degrees in electronic and information engineering from the South China University of Technology, Guangzhou, China, in 2011 and 2014, respectively, and the PhD degree from the Electrical and Electronic Engineering Department, Imperial College London, U.K., in 2018. He is currently an associate professor with the College of Cyber Security, Jinan University, Guangzhou, China. He is the recipient of the 2021 CIE Information Theory Society Yong-star Award, and the 2020 superstar supervisor award of the



Processing, CVPR, ICCV, ICDM, Pattern Recognition, Information Sciences, Cognitive Computation and Neucomputation.

Xiaobo Jin is currently an associate professor in Intelligent Science Department, School of Advanced Technology, Xi'an Jiaotong-Liverpool University. He graduated from Pattern Recognition and Intelligent System from National Laboratory of Pattern Recognition, Institute of Automation, Chinese Academy of Sciences, whose interests lie in the areas of machine learning and computer vision. He has published over 60 papers including international authoritative journals and conferences such as IEEE Transactions on NLS, IEEE Transactions on Image